MAXIMUM RECOVERY AREA IN APPROACH FOR THE SPACE PLANE HERMES*

F. Jouhaud

Office National d'Etudes et de Recherches Aérospatiales
92320, Châtillon (France)

Abstract

The global performances of the spaceplane HERMES in approach (altitude below 25 km, Mach below 2) are evaluated by the determination of maximum recovery areas. For one given initial azimuth, each maximum recovery area is the set of points wich allow to reach the runway with respect to all the constraints (load factor, longitudinal equilibrium,...). Each point of the boundary of the area is obtained by means of optimization of a trajectory maximizing the approach distance in a particular azimuth.

The singular perturbation technique has been successfully used to solve this optimal problem : not only the boundaries of the recovery area for different initial azimuths were computed but also the effects of aerodynamic dispersions, supplementary constraints, presence of wind were studied.

I. INTRODUCTION

In order to qualify the global performances of the space plane "HERMES" (European project of a space shuttle), and to estimate the requirements for the guidance system during hypersonic reentry, it is necessary to compute the maximum recovery area in approach. This area is defined as the set of points from where, for a given velocity (Mach $\leq$ 2), altitude h (h $\leq$ 30 km) and azimuth, it is possible to reach the landing runway, while fulfilling all the constraints (longitudinal equilibrium, maximum load factor and dynamic pressure,...).

Each point of the boundary of this area can be determined by optimization of a trajectory maximizing the distance in a given azimuth towards the runway. The exploration of this azimuth allows to build the whole boundary of the area.

One method has been particularly investigated for this study : the singular perturbations technique (SPT) [1, 2, 3].

The SPT leads to an approximate resolution by splitting time scale among the state vector. For HERMES, velocity and horizontal location are assumed to be varying slowly, altitude and flight-path angle quickly, and azimuth is intermediary. This dynamic decomposition yields an analytical solution for the controls.

The so found trajectory (by the SPT) is afterward used as an initial trajectory for a numerical optimization method (generalized projected gradient [4]). The trajectory, obtained by this last method, is used as a reference for comparisons.

*This research was supported by the Centre National d'Etudes Spatiales (CNES)

Copyright © 1988 by ICAS and AIAA. All rights reserved.

II. MAXIMUM RECOVERY AREA PROBLEM

II.1. Equations of motion of spaceplane

The flight of the spaceplane in terminal phase (with altitude below 30 km and Mach $\leq$ 2) is described with the following assumptions :

i) the Earth is fixed and flat, gravity acceleration is constant (g = 9.81 m/s^2).

ii) the flight is performed without side-slip.

iii) the transients on attitude motion are neglected.

The control variables are the attack angle α and the aerodynamic banck angle μ. α is defined as the angle between velocity vector and fuselage axis ; bank angle μ is given by the angle between the symmetry plane and the vertical plane containing the velocity vector $\vec{V}$ (see Fig. 1).

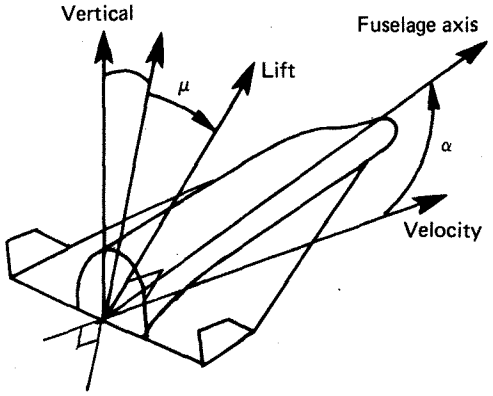

Fig. 1 — Definition of angles α and μ.

The spaceplane is located by its horizontal position (x towards North, y towards East), and altitude (h). The velocity vector is defined by its components : modulus V, flight-path angle γ (positive if V is above an horizontal plane) and azimuth χ in regard to North (positive if Eastward).

With those assumptions, the equations of motion of the space plane are [5] :

$$\left[\begin{array}{ll} \frac{dx}{dt} = V\cos\gamma\cos\chi & \frac{dV}{dt} = -g\left(\sin\gamma + \frac{n_z}{f}\right) \\ \frac{dy}{dt} = V\cos\gamma\sin\chi & \frac{d\gamma}{dt} = -\frac{g}{V}\left(\cos\gamma - n_z\cos\mu\right) \\ \frac{dh}{dt} = V\sin\gamma & \frac{d\chi}{dt} = \frac{g}{V}\, n_z\, \frac{\sin\mu}{\cos\gamma} \end{array}\right. \quad (1)$$

where :

$f = C_L/C_D$: lift to drag ratio, with C_L and

C_D respectively lift and drag coefficients ;

$n_z = \frac{1}{2} \rho V^2 \frac{S C_L}{m g}$: normal lead factor with

ρ : mass density of atmosphere at altitude h,

m : mass of vehicle,

s : reference area.

As the relation $n_z (C_L(\alpha))$ can be inverted to provide $\alpha (n_z)$, the lift to drag ratio f is a function of nz, therefore nz can be conveniently used as a commande instead of the attack angle.

II.2. Formulation of the maximum recovery area problem

Let us recall that the maximum recovery area (MRA) is the set of space points, defined by its horizontal coordinates (x, y) at a fixed altitude, from where the space plane can reach and land on the runway. At the begining of the terminal phase, that is at the end of the hypersonic reentry, azimuth χ_o and Mach number, or equivalently total height $H_o = h_o + V_o^2/(2g)$, are well defined.

By another way, in order to land on the runway with appropriate safety conditions, the spaceplane must reach the vertical plane along the runway axis, at a given distance and height from the runway threshold, with specified velocity and flight-path angle.

More precisely, the final state vector of the space plane is fully specified by the following landing conditions :

- altitude of 3 km ;
- velocity
- flight-path angle } fixed,
- azimuth equal to that of runway : χ_r ,
- horizontal position on the runway axis, at 10 km of the runway threshold.

For same reasons of safety, the space plane trajectory must also satisfy following current constraints :

- normal load factor nz $\leqslant$ 2.5,
- conventional velocity $V_c \leqslant$ 165 m/s (320 kTs).

The determination of a MRA, related to a fixed initial azimuth χ_o , is obtained by seeking a family of optimal trajectories by proceeding in the two following steps :

i) we search the optimal trajectory which allows to reach the runway from an initial horizontal position (x_o , y_o) as far as possible the azimuth χ_a , as can be seen on Figure 2.

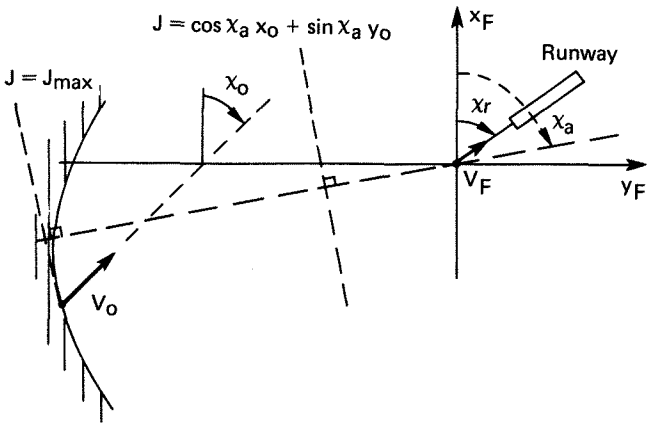

Fig. 2 – Approach configuration.

The cost function to be maximized is then the horizontal distance along direction χ_a , wich can be written as :

$$J = \cos \chi_a \; x_o + \sin \chi_a \; y_o \qquad (2)$$

ii) The boundary of the MRA, related to initial azimuth χ_o is got by varying the azimuth χ_a. The whole set of MRA is afterward obtained by changing the value of χ_o.

II.3. Optimal control problem

By application of Pontryagin's principle [2], it is well known that the optimal controls nz and μ must minimize the Hamiltonian H associated to (1) and (2) :

$$n_z^* , \mu^* = \underset{n_z , \mu}{\text{Arg Min}} \; H(n_z , \mu) \qquad (3)$$

with :

$$H = p_x V \cos\gamma \cos\chi + p_y V \cos\gamma \sin\chi + p_h V \sin\gamma - p_V g \left(\sin\gamma + n_z / f\right) - p_\gamma \frac{g}{V} (\cos\gamma - n_z \cos\mu) + p_\chi \frac{g}{V} \frac{n_z \sin\mu}{\cos\gamma} \qquad (4)$$

In this relation (4), the adjoints variables P_x, Py, Ph, P_V , P_γ, P_χ satisfy the following equations :

$$\begin{cases} \frac{dp_x}{dt} = 0 \;, \quad \frac{dp_y}{dt} = 0 \;, \quad \frac{dp_h}{dt} = p_V \, g \, n_z \, \frac{\partial}{\partial h}\left(\frac{1}{f}\right) \\ \frac{dp_V}{dt} = -p_x \cos\gamma \cos\chi - p_y \sin\chi \cos\gamma - p_h \sin\gamma + p_\gamma \frac{g}{V^2}(n_z \cos\mu - \cos\gamma) + p_\chi \frac{g}{V^2} n_z \frac{\sin\mu}{\cos\gamma} + p_V \, g \, n_z \, \frac{\partial}{\partial V}\left(\frac{1}{f}\right) \\ \frac{dp_\gamma}{dt} = p_x V \cos\chi \cos\gamma + p_y V \sin\chi \sin\gamma - p_h V \cos\gamma + p_V g \cos\gamma - p_\gamma \frac{g}{V} \sin\gamma - p_\chi g \frac{n_z}{V} \frac{\sin\mu \sin\gamma}{\cos^2\gamma} \\ \frac{dp_\chi}{dt} = p_x V \sin\chi \cos\gamma - p_y V \cos\chi \cos\gamma \end{cases} \qquad (5)$$

with the final conditions :

$$\begin{cases} p_x(t_f) = -\cos\chi_a & p_V(t_f) = \lambda_V \\ p_y(t_f) = -\sin\chi_a & p_\gamma(t_f) = \lambda_\gamma \\ p_h(t_f) = \lambda_h & p_\chi(t_f) = \lambda_\chi \end{cases} \qquad (6)$$

where λ_h , λ_V , λ_γ , λ_χ are Lagrangian multipliers associated, respectively, with the final constraint, on h , V , γ and χ .

Let us notice that, as the system (1) does not depend explicitely of time t, the Hamiltonian, associated with optimal controls nz* and μ^*, satisfies the condition [6] :

$$H(n_z^* , \mu^*) = 0 \qquad (7)$$

The solution of such an optimal control problem involves the well known two-points boundary value problem, and requires specific numerical iterative methods.

In order to minimize the amount of computational time (which is also usefull for guidance purpose), an approximate, but quasi-analytical, solution has been seeked by means of the singular perturbation technique.

III. APPLICATION OF THE SINGULAR PERTURBATION TECHNIQUE TO OPTIMAL CONTROL

The SPT [1, 2, 3] is an approximate method of resolution of a differential system of

equations. It is based on the existence of several time-scale on the state variables. Typically, for a linear system, this implies that there is large differences between the eigenvalues of the system.

For the flight of the space plane HERMES, the dynamic is assumed to have the following time scales : the horizontal position x, y and the velocity V are "slow" variable, while altitude h and flight-path angle γ are "fast" variables and azimuth χ is an intermediary variable. Naturally, this assumption is to be verified afterwards by comparisons with solutions provided by numerical optimization technique.

The equations (1) are rewritten in a singularly perturb form as follows [5].

$$\begin{cases} \dfrac{dx}{dt} = V\cos\gamma\cos\chi \\ \dfrac{dy}{dt} = V\cos\gamma\sin\chi \\ \dfrac{dV}{dt} = -g\left(\sin\gamma + \dfrac{n_z}{f}\right) \end{cases} \qquad \begin{cases} \varepsilon\dfrac{d\chi}{dt} = \dfrac{g}{V} n_z \dfrac{\sin\mu}{\cos\gamma} \\ \varepsilon\dfrac{dh}{dt} = V\sin\gamma \\ \varepsilon\dfrac{d\gamma}{dt} = -\dfrac{g}{V}(\cos\gamma - n_z\cos\mu) \end{cases} \tag{8}$$

ε is a small parameter wich is artificially introduced to separate the time scale between (x, y, V), (χ) and (h, γ).

The above assumption on time-scale separation between different state variables induces the same time-scale separation between the corresponding adjoints variable in equations (5).

A zeroth-order solution of the singularity perturbed optimal control problem, given by equation (8), is obtained by solving firstly the reduced problem wich is defined by setting ε = 0 in equation (8).

The so obtained solution is called "outer solution" or "reduced solution".

Nevertheless, this solution introduces discontinuities on initial and final conditions on the fast variables (χ, h and γ).

The "matching" of these fast variables is obtained through two "boundary-layers", related to the intermediate variable χ and to the fast variables h and γ .

THe global control laws of the system (8), of close-loop type, is then given by the solution provided by the last "boundary-layer" problem, by using the "reset" technique.

Nevertheless, for purpose of the computation of maximum recovery area, some further simplifications are also considered.

The detailed description of the solution is given below.

III.1. Outer solution

Assuming that ε is a "small" parameter, an approximate solution is obtained by setting ε = 0 in the equation (8) and the problem can be solved analytically.

This outer solution corresponds to a trajectory such that [5] :

$$\begin{cases} \bar{n}_z = 1 \quad , \quad \bar{\mu} = 0 \\ \bar{\gamma} = 0 \quad , \quad \bar{\chi} = \chi_a \\ \bar{h}(V) = \mathrm{Arg}\,\max_h (\bar{f}) \\ \bar{p}_x = -\cos\chi_a \quad , \quad \bar{p}_y = -\sin\chi_a \\ \bar{p}_V = -\dfrac{\bar{V}}{g}\bar{f} \end{cases} \tag{9}$$

$\bar{h}(V)$ can be computed off-line end stored as a one-dimensional table. For HERMES this descent profile is indicated on Figure 4.

The outer solution is a plane trajectory where HERMES is flying with the selected approach azimuth χ_a with maximum lift to drag ratio, at such an altitude that load factor nz is equal to unity.

III.2. Initial boundary layer in azimuth χ

The time is streched near initial time by the transformation $t_1 = (t - t_0)/\varepsilon$ in (8). Then, by setting ε = 0, the slower variables are frozen to their initial value ($\hat{x} = x_0$, $\hat{y} = y_0$, $V = V_0$), while we have for the azimuth the following equation [5] :

$$\frac{d\hat{\chi}}{dt} = \frac{g}{V_0}\hat{n}_z \sin\hat{\mu} \quad , \quad \hat{\chi}(0) = \chi_0 \tag{10}$$

with

$$\begin{cases} \hat{n}_z = \dfrac{1}{\cos\mu} \quad , \quad \dfrac{\cos\mu}{\hat{f}} = \dfrac{\cos(\hat{\chi} - \chi_a)}{\bar{f}_0} \\ \hat{\gamma} = 0 \\ \hat{h} = \mathrm{Arg}\,\max_h (\hat{f}) \\ \hat{p}_\chi = \bar{p}_{V_0} V_0 \dfrac{\sin\hat{\mu}}{\hat{f}} \end{cases} \tag{11}$$

As the Mach number is varying slowly with the altitude (for a given velocity), we have approximately $\hat{f} \simeq f_0$ and then we deduct :

$$\begin{cases} \hat{\mu} \simeq \chi_a - \hat{\chi} \\ \hat{\rho} \simeq \dfrac{\bar{\rho}}{\cos\hat{\mu}} \end{cases} \tag{12}$$

The initial boundary layer (IBL) in azimuth corresponds to a turn from the initial azimuth χ_0 to the azimuth χ_a of the outer solution.

This turn is performed with maximum lift to drag ratio, at an altitude, for a given speed, lower than for the outer solution.

III.3. Initial boundary layer for altitude and flight-path angle

The goal of this second initial boundary layer is to fit the initial values of altitude and flight-path angle to the "outer" values of h and γ , these values being given by the initial boundary layer in azimuth.

As only the total height is fixed, we can choose the set ($\bar{h}_0$, $\bar{V}_0$) in order to respect this total height (see Fig. 4) as initial conditions ; and as the flight-path angle of both outer solution and first IBL is irrelevant ($\bar{\gamma} = \hat{\gamma} = 0$), the adjustment of flight-path angle is also ignored.

III.4. Final boundary layer in azimuth

The time is stretched near the final time by the transformation $t_2 = (t_f - t)/\varepsilon$ in (8). The equations obtained are identical to those of IBL in azimuth, with χ_0 replaced by χ_r (χ_r is the landing azimuth of runway).

Nevertheless, due to difficulties encountered with SPT for fulfilling the final boundary-layers (FBL), it has been preferred to switch from the outer solution to the FBL in azimuth at an a priori altitude, function of the

difference between approach and landing azimuth : $\chi_a - \chi_r$. For this purpose, the bank angle μ was set equal to $\chi_r - \chi$.

III.5. Final boundary-layer in altitude and flight path- angle

As for the FBL in azimuth, the same difficulties arise, but as altitude and flight-path angle are the fastest variables, the correction of the FBL will occur only at the end of the trajectory, with little influence on the approach distance under maximization. So this FBL is ignored.

III.6. Summary of the control laws

The first computationnal tests have shown that a further simplification of the expression of controls can be achieved in selecting for a given point of the trajectory :

- attack angle corresponding to maximum lift to drag ratio,
- bank angle equal to the difference between target and current azimuth. The target azimuth is initially the approach azimuth χ_a and close to the final altitude, it is switched to runway azimuth χ_r.

IV. RESULTS

The method previously described has been applied to the space plane "HERMES", with its aerodynamic coefficients, function of Mach number and attack angle.

In order to qualify the results of the SPT, a comparison has been done with the solution provided by a numerical optimization method : the generalized projected gradient (GPG) [4], without taking into account the approximation of time-scale separation as previously.

The GPG is an original method developed at ONERA. It is an extension of the classical projected gradient technique, allowing simultaneously the optimization of a choosen performance and the satisfaction to all the given constraints, while giving priority to the last ones. Unlike many other numerical optimization methods, the GPG fits easily for numerous, varied constraints, even if they are not satisfied for the initial trajectory.

In order to reduce the computationnal time with this numerical method, the trajectory provided by the SPT has been used as the initial trajectory for the GPG.

As expected, the results show a good agreement between the two trajectories obtained by the two methods, with a discrepancy at the end of trajectories, because the numerical provided by the GPG fulfill all the final constraints on state variables.

This discrepancy does not affect the approach distance under maximization, since the two methods agree within one percent.

Moreover, thanks to the great proximity of the SPT trajectory compared to the optimum, the GPG had only a few iteration to perform, typically 20.

Figure 3 shows the maximum recovery area corresponding to an initial azimuth equal to that of runway.

Figures 5 to 9 display the evolution, respectively, of σ_1/μ versus t, h versus V, h, V, nz, σ versus t for the recovery trajectory related to approach direction $\chi_a = \chi_r + 90°$ and with initial $\chi_o = \chi_r$, and designed by the symbol "*" on figure 3.

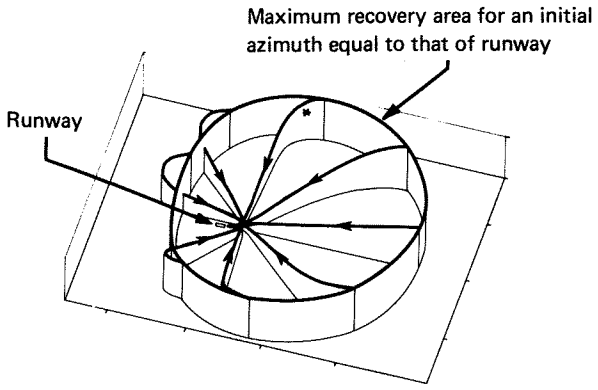

Fig. 3 — Perspective view of a maximum recovery area.

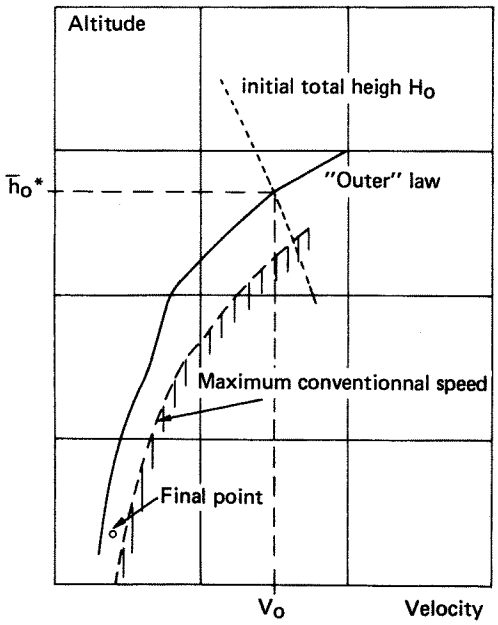

Fig. 4 — Outer law of altitude.

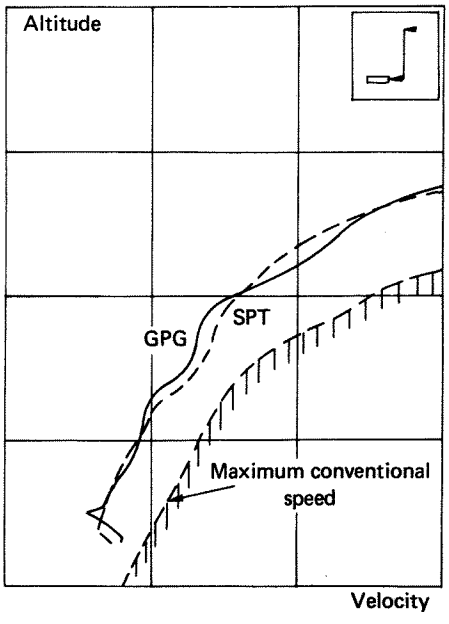

Fig. 5 — Typical recovery trajectory, altitude versus velocity.

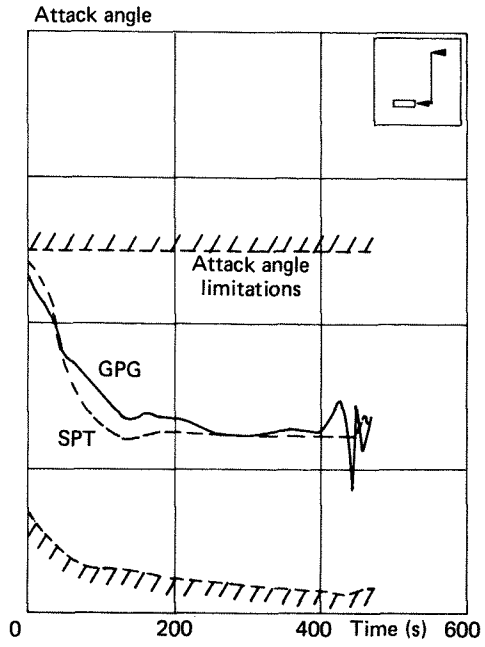

Fig. 6 – Typical recovery trajectory, attack angle versus time.

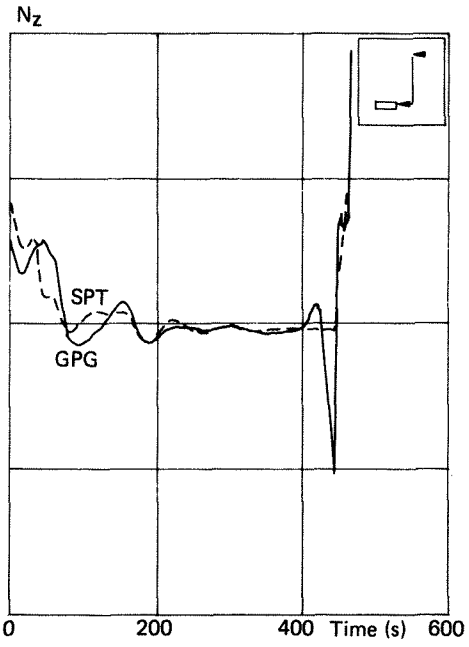

Fig. 8 – Typical recovery trajectory, N_z versus time.

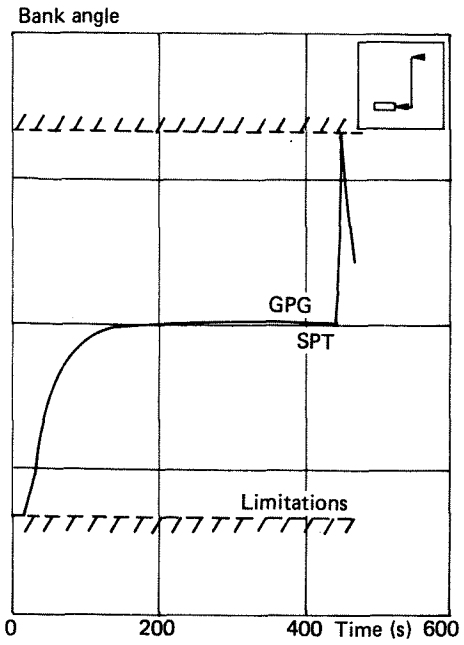

Fig. 7 – Typical recovery trajectory, bank angle versus time.

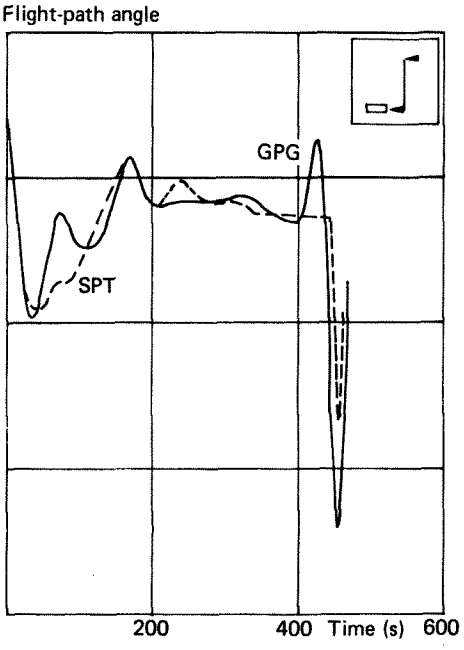

Fig. 9 – Typical recovery trajectory, flight-path angle versus time.

Thanks to the quasi-optimality of the SPT method, a great number of cases have been treated. Not only the boundaries of the maximum recovery initial azimuth have been computed, but the effect of several dispersion causes has also been investigated.

These were (see Table 1) :
- effect of aerodynamic perturbations : lift to drag ratio lower or higher than nominal case, speed-brakes set out ;
- effect of initial flight-path angle ;
- effect of initial altitude ;
- lower allowed normal load factor ;
- velocity continuously decreasing ;
- limitation of flight-path angle ;
- wind effect at Istres (France) and Kourou (Guyane).

Table 1 — Dispersion effects.

Cause of dispersion	Mean effect on approach distance
Lift to drag ratio - 10 %	- 15 %
Lift to drag ratio + 25 %	+ 27 %
Speed brakes set out	- 13 %
Initial flight-path angle reduced of 6°	- 3 %
Initial altitude reduced of 2.5 km	- 2.3 %
n_z max = 2 instead of 2.5	- 0.2 %
Velocity continuously decreasing	- 1.5 %
Flight-path angle > - 20°	- 3 %
Wind profile at Istre (France)	- 9 %
Wind profile at Kourou (Guyanne)	- 1 %

V. CONCLUSION

The singular perturbation technique (SPT) has allowed to perform a quasi-analytical resolution of the Pontryagin's principle applied to the problem of the maximum recovery area of HERMES in the terminal phase.

The control law found were simple : angle of attack corresponding to maximum lift to drag ratio, bank angle equal to the difference between the current azimuth and the target azimuth.

In comparison with an "exact" optimal solution given by a numerical iterative optimization method (generalized projected gradient, GPG), the SPT has provided relatively very accurate solutions, since the approach distance under maximization was in good agreement with GPG solution, within one percent.

Regarding to the simplificity and accuracy of these singularly perturbed control laws, a great number of cases have been carried out : computation of maximum recovery areas for different initial azimuths, influence of aerodynamic dispersions, additional constraints, influence of wind.

REFERENCES

[1] W. Wasow
Asymptotic Expansions for Ordinary Differential Equations.
Interscience publishers, J. Wiley and Sons, New-York (1965).

[2] M.D. Ardema
Singular Perturbations and Control.
CISA Courses and lecture n° 280 - Springer-Verlag - Wien - New-York (1983).

[3] M. Dokhac - H.T. Huynh
Determination des Lois de Guidage en "Temps Réel" pour des Avions d'Armes en Interception Tridimensionnelle.
ONERA - RT n° 29/514854 (1986).

[4] C. Aumasson - P. Landiech
Methode du Gradient Projeté pour l'Optimisation Paramétrique et Fonctionnelle de Systèmes Dynamiques Soumis à des Contraintes.
ONERA - RT n° 22/6115 (1987).

[5] F. Jouhaud
Domaine Maximal de Recueil d'HERMES en Phase Terminale.
ONERA - RT n° 4/6121SY (1987).

[6] L.S. Pontryagin - V.G. Boltyanskii - R.V. Gamkrelidze - E.F. Nischchenko. The Mathematical Theory of Optimal Processes.
Interscience Publishers, J. Wiley and Sons, New-York (1962).